CHARACTERIZATION OF DAMAGE IN CrMoV STEEL BY APPLICATION OF X-RAY MICRO-TOMOGRAPHY

C. Gupta[1#], J.K.Chakravartty[1], and A. K. Suri[2]
[1]Mechanical Metallurgy Division, Materials Group, Bhabha Atomic Research Centre, Mumbai, INDIA-400085.
[2]Materials Group, Bhabha Atomic Research Centre, Mumbai, INDIA-400085.
Corresponding is author on sabbatical with Department of Mechanical Engineering, Toyohashi University of Technology, Toyohashi, AICHI, JAPAN
E-mail of corresponding author:joy_gupta71@yahoo.co.in

ABSTRACT

The presence of voids in the necked region of CrMoV steel for nuclear applications were imaged and characterized using Micro-focus X-ray computed tomography. The samples of two different cross-sections for micro-tomography were extracted from tensile deformed specimens, interrupted at the formation of local neck. The tomography scan on the deformed sample were then compared with that of the un-deformed sample to quantitatively characterize the spatial void distribution in terms of their size, shape and volume fraction using commercially available software. The nature of the voids was found to be predominately rod shaped structures with very low sphericity.

INTRODUCTION

Damage in structural steels for high performance applications such as nuclear power plant structural components is inevitable during service. As a result the technological properties such as strength, ductility and fracture toughness are adversely affected [1,2]. The final stages of failure in most cases are associated with creation of voids and their final manifestation into cracks by void coalescence [2]. Thus the tendency of failure by means of phenomena such as ductile fracture, depends on the ability of the structural material to resist not only the creation of defects such as voids but also their proliferation and accumulation in the structure [2]. Conventional tools used to characterise the void distribution, such as scanning electron microscopy and transmission electron microscopy have been largely invasive in nature [1]. Further, these techniques require elaborate sample preparation and yields very little volumetric information. As a result various phenomenological relations predicting degradation of functional properties of structural materials such as steels, based on damage evolution approach, depend on the ability of sample preparation technique to preserve the integrity of void structure developed as a result of damage process. X-ray micro-tomography (μ-CT) has emerged in recent times as a tool to evaluate non-destructively in a quantitative manner the internal structure of materials [3, 4]. The tremendous interest in the application of X-ray based tomography techniques is due to the ability to give 3-D images of the internal structure of materials in a non-invasive manner [3, 4]. The development of X-ray micro- and nano- tomography techniques to enable non-destructive characterization of internal structures of materials has been enabled by the availability of high brilliant sources of third generation synchrotron radiation with excellent lateral coherence and monochromaticity (eg. ID19 beam line of the European Synchrotron Radiation Facility [5], Grenoble France (lateral coherence ~ 100μm and wavelength 0.5 $\overset{o}{A}$)), advances in detector technologies [6], availability of high performance desk top computing, developments in reconstruction algorithm such as cone beam reconstruction [3] and by the development of sensitive contrast mechanisms such as phase contrast technique[3,7,8]. The desktop systems have also concomitantly been upgraded to be capable to give sub-micron and nano-scale resolution with the development of micro-focus x-ray sources and large format detectors [9-11]. As a result the recent literature has increasingly seen research into understanding the failure mechanisms of modern structural materials such as metal matrix composites [12,13], foams [14], aluminum alloys [15] etc. on the basis of 3-D images during the development of various types of internal damage – voids and their coalescence, and micro-cracks and their propagation [16-21]. More conventional structural materials such as steels impose a challenging environment to carry out tomography as they have a high linear attenuation coefficient (LAC) and consequently require higher incidence beam energies in order to achieve adequate penetration of sample volume containing representative defect content. While X-ray μ-CT to characterise the internal defect structure has been used for potential structural materials such as foams and composites, it has been seldom applied to steels which possess high linear absorption coefficient (LAC) that results in poor resolution of the internal defect structure, especially at input energy levels in the photoelectric domain. Therefore for steels the application of tomography has been extremely limited, especially at incidence X-ray energy levels where 'Z'

(atomic number) contrast is dominant [3, 22, 23]. In this work micro-focus X-ray CT technique has been successfully applied for the first time to a conventional structural steel, deformed in the tensile mode to reveal the details of internal defect structure in the necked region.

EXPERIMENTAL

The tensile sample of 4.01 mm diameter and 20 mm gage length of a low alloy steel for nuclear reactor pressure vessel application (3Cr-0.75Mo-0.25V) steel was deformed in servo-hydraulic test machine until necking in the sample was well developed, after which the test was interrupted and sample unloaded. From the necking region two types of samples with different cross-section geometry were made that was to be subjected to tomography scan. The first sample type was made from the partially necked sample by 'coring' out a central square section of dimensions of about 500µm x 500µm along the gage of the specimen including the necked portion of the sample. The second type of sample was made from the sliced-out, side-portion that remained during the process of coring out the central square section. The slice cut enclosed the neck section (shown in inset of figure 1(a)) and was further mechanically ground to 430 µm thickness. A third sample was prepared from the gage section of the un-deformed specimen of the Cr-Mo-V steel in the same way as the first sample. The X-ray tomography scan was carried out on these samples as described below.

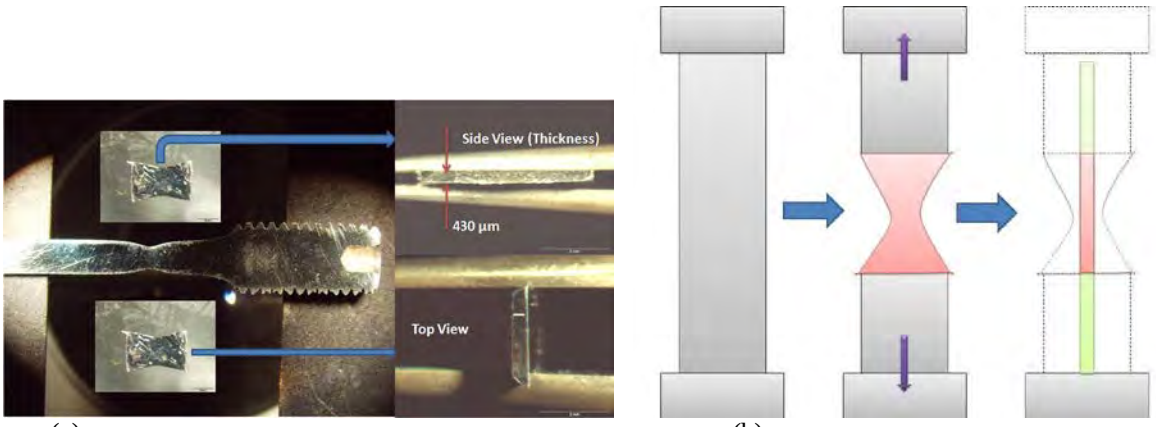

(a) (b)

Figure 1 (a) Stereo-micrograph images of the sample with rectangular cross-section showing the cut away view after the coring operation. The side view and the top view of the sample after mechanical grinding operation to a thickness of 430µm has been also shown. (b) Schematic showing the steps in preparation of sample containing voids for the tomography scan.

The Skyscan 1172, a high resolution desk top X-ray micro-tomography scanner, was used for obtaining virtual slices from the different samples. The scanning was carried out at a maximum power of the X-ray micro focus tube i.e. 100kV and 100µA current, which resulted in the photon energies to lie in the domain where LAC strongly depends on density and atomic number of the material [3]. As a result of LAC being sensitive to both density (ρ) and atomic number (Z, and proportional to Z^4), the imaging of defect interfaces (predominately consisting of voids) would be facilitated by strong contrast developed due to the product ρZ^4 tending to very small values for voids in comparison to the surrounding steel in which they are embedded. A filter of Al+Cu was used to reduce the beam hardening artifacts that arise with the use of polychromatic beam source. This filter and the fact that a dense sample has to be imaged lead to an exposure time of 3540 ms. The sample was rotated 360° with scanning recorded at intervals of 0.4° on a CCD detector with 1048 x 2000 pixels. The source – detector – sample distances were suitable arranged to give an image pixel size of 1.5 µm for the deformed square sample and 1.745 µm for the un-deformed square sample and sample slice containing the neck. The reconstruction of the 16 bit projection images was carried out using commercially available software "NRecon" based on the modified feldkamp algorithm. The final reconstructed images were converted to 8 bit gray scale format.

RESULTS & DISCUSSION

The stress strain curve obtained from the tensile test carried out on the CrMoV steel has been shown in figure 2. The test was interrupted when necking was developed with a reduction in area reaching 32.67%. The yield stress of the material at room temperature was 600 MPa and ultimate tensile strength 713 MPa (at uniform elongation = 0.067). Using Bridgeman correction due to neck formation on the basis of empirical estimation of neck geometry (c.f eq 6.10 [2]), the stress at the minimum section was estimated to be 742 MPa (c.f eq 6.9 [2]). The inset shows a close up view of the necking profile and also the final sample that was subjected to the tomography experiment.

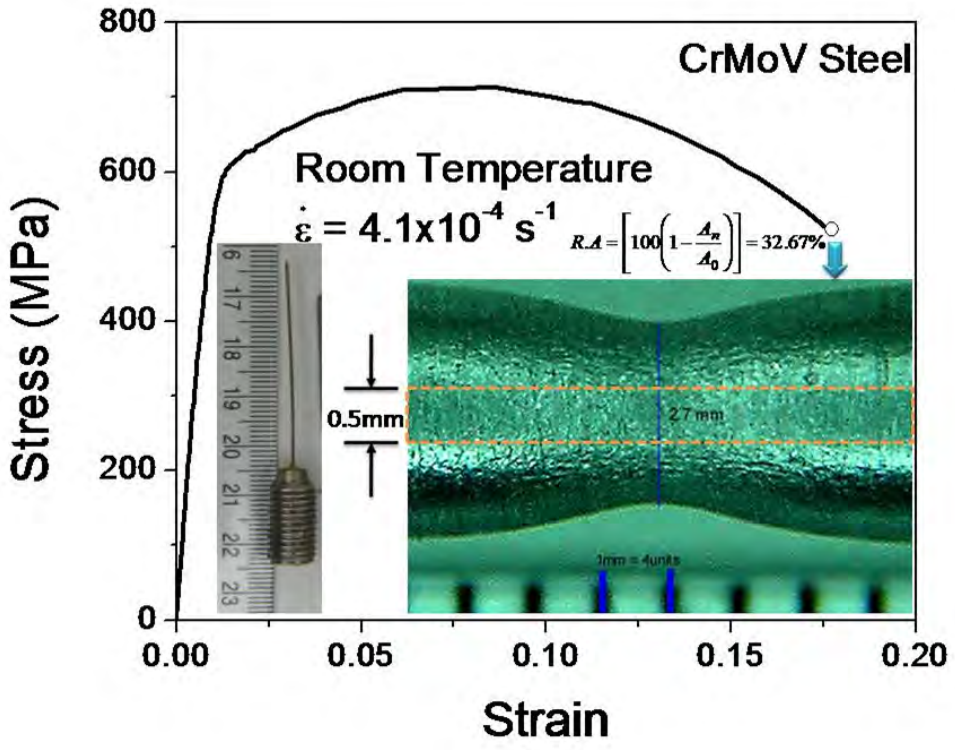

Figure 2. Stress – Strain plot of the sample subjected to the tomography scan. The inset shows the necked potion and the final sample with square cross-section machined from the tested specimen that was used for tomography.

The results of the tomography scan on the deformed and un-deformed samples with square cross-section have been compared in figure 3. The images shown are from slice section stack of 200 slices made using the software ImageJ [23]. It is seen that the images do not show the presence of internal defects. However, the profile of gray scale intensity in the images shows significant differences. The gray scale profile as a function of pixel across the midsection for the deformed sample consistently shows higher intensity as compared with the un-deformed sample. It is well known that in absorption tomography the reconstructed images basically represent the spatial distribution of the attenuation coefficients in the image volume. These are then linearly mapped to an appropriate grey scale depth dictated by the image format (i.e. 16 bit or 8 bit) in which they are viewed. Therefore differences in the grey scale represent the differences in attenuation coefficients. The fact that grey scale profile for the deformed sample is higher across the sampled line as compared with the un-deformed case, means that the attenuation in the former is higher. It is also seen from the figures that there is sample size difference between the two with the un-deformed sample being the larger one among the two. Thus one can conclude from these results that in smaller sample containing de-cohesion damage in the form of voids the attenuation is larger. This is also seen in the figure 4

showing the distribution of the attenuation coefficients along the sample diagonal for the two samples. The average attenuation coefficient is slightly higher for the smaller deformed sample. This is an unexpected result as the presence of defects such as voids would reduce the LAC of the steel. This can be probably rationalized as being due to the fact that the scattering interfaces of void surface provide additional factor to increase the absorption of in-coming photons locally, compounded by the presence of particles in their vicinity and a sample thickness that is too large for the scattered photons to escape. The fact that pore/void interfaces in steel display a bright 'halo' during combined absorption and phase contrast imaging with monochromatic synchrotron radiation beam [24] provide plausible reasons for them to scatter photons with polychromatic beam in absorption tomography. The secondary absorption of the scattered photons at particles cannot also be ruled out. The above could mean that a thinner sample would be better suited to image voids embedded in the volume. Hence a thinner sample was scanned, the results of which are indicated below.

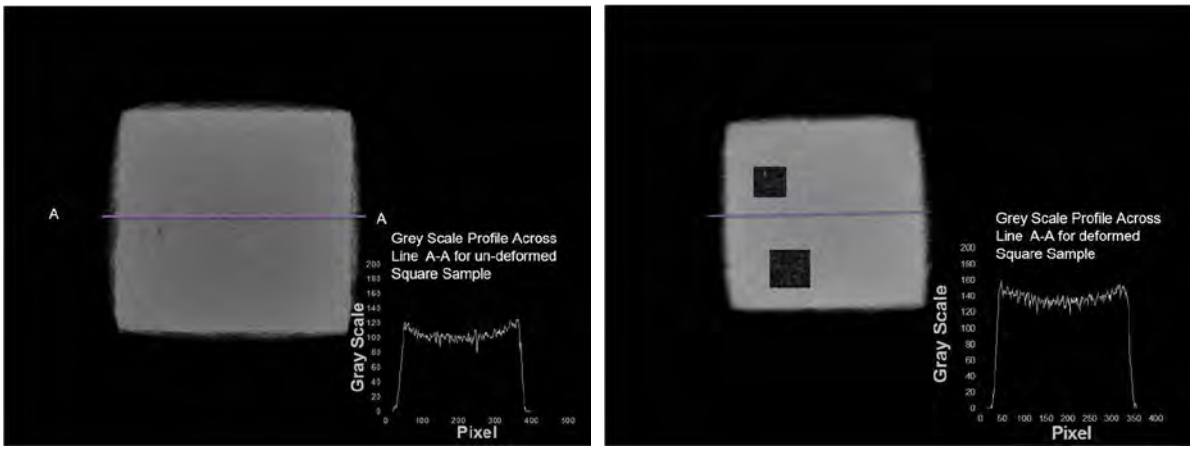

(a) (b)

Figure 3. Tomography scan slices from the square cross-section samples that has (a) not been deformed (b) been subjected to deformation. The inset of each also shows the plot of variation of the intensity profile across the line A-A for comparison. The sampling line length A-A for un-deformed sample image is 727 μm and 576 μm for the deformed sample image.

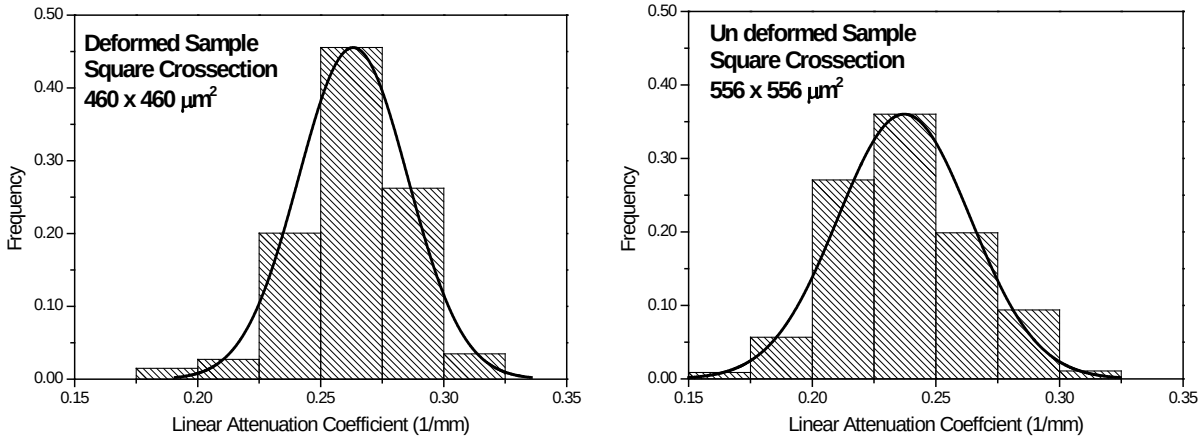

(a) (b)

Figure 4. The distribution of the linear attenuation coefficient across the diagonals of the samples with square crossection for the (a) deformed sample (b) not deformed sample.

The images obtained from the tomography scan of the thinner rectangular cross-section sample containing the neck, and processed in ImageJ [24] to form a stack of slice sections and its corresponding coronal view, are shown in figure 5. It is clearly seen in both the views that the section contains many discolored/dark areas. These dark areas (seen in the slice section / light areas in the coronal view due to inversion operation of the gray scale image) are location where the X-ray intensity has suffered significant loss. The void surfaces as already pointed out are highly scattering interfaces and therefore hinder the passage of photons resulting in sharp attenuation in the vicinity of voids. The gray scale profile across the indicated line section in the coronal view clearly shows the discolored areas represent areas of low intensity. The low intensity areas in the image have been shown in light discolored regions as the gray scale has been inverted. A portion of the coronal and the slice section stacks have been processed to find the gradient in the local region, using ImageJ software, which implements a 2D sobel filter mask for the purpose of calculating the gradient of the images. These are indicated in the respective figures as region B and C. It is seen that the void interfaces after implementation of the gradient calculation are clearly revealed both in the slice section and the coronal view. While in the slice section stack these are rounded in shape in the coronal image these are elongated structures in the direction of tensile stress. This is expected as the slice sections are taken in a plane normal to the direction of the applied stress and the coronal view is parallel to it. The linear attenuation distribution in the X- and Y- directions of the thin rectangular sample is shown in figure 6. The mean attenuation is slightly lower than those of the sample with square cross-section, where the voids were not visible at all. Thus it appears from present study that the asymmetric cross-section has facilitated the reduction of attenuation coefficient and imaging of voids. Further investigations are required to clarify the underlying factors for this observation.

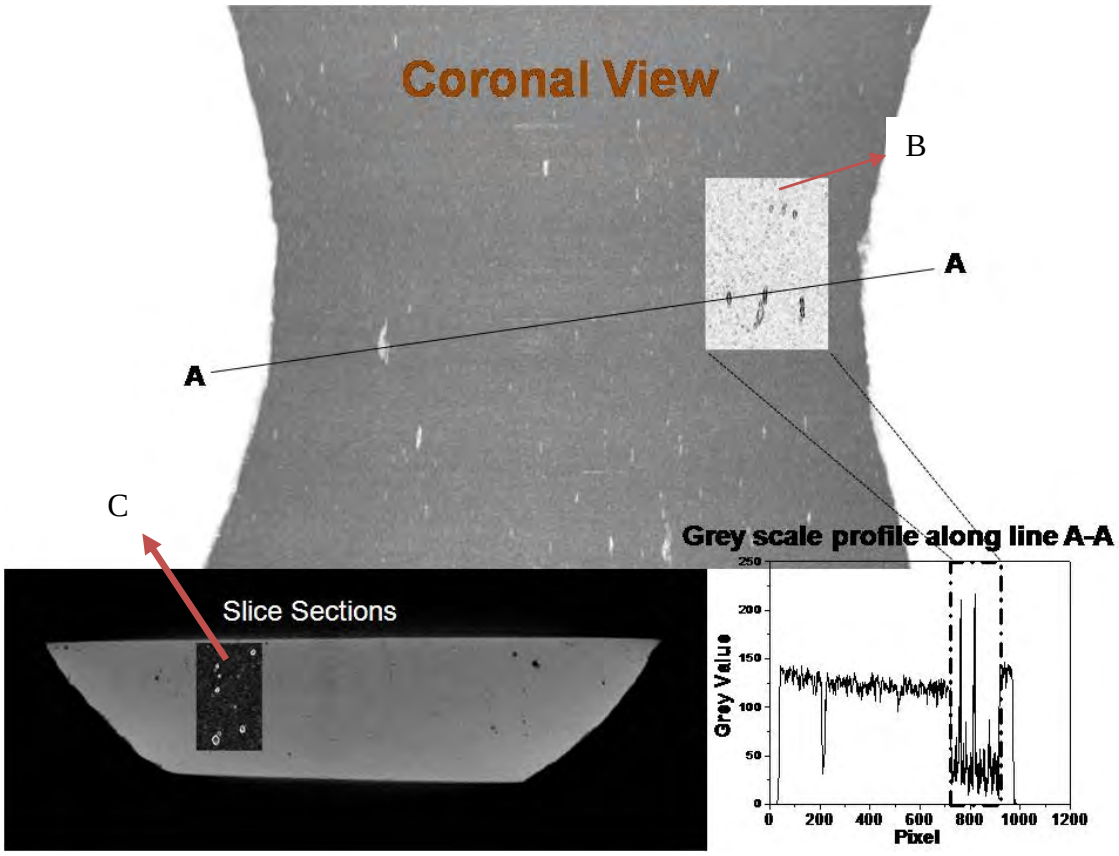

Figure 5. Tomography scan slice obtained in Grey scale format (in inverted scale) showing the cross-sectional slice stack and the corresponding coronal view slice stack. Regions B and C indicate the local regions where the gradient of the image has been determined to clearly delineate the location of voids in the slice. The plot of gray scale intensity with pixel along the profile A-A has also been shown.

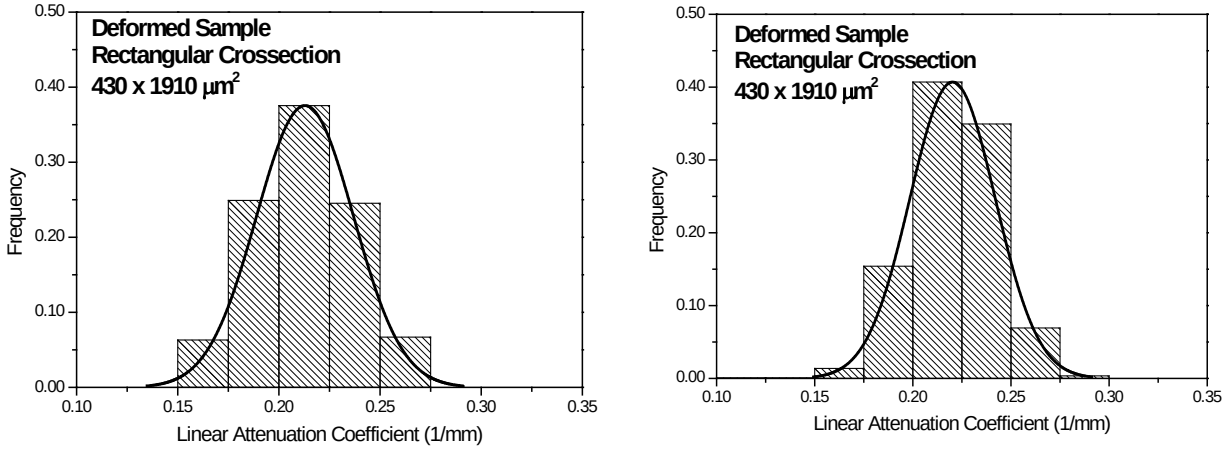

(a) (b)

Figure 6. The distribution of the linear attenuation coefficient along the (a) X- direction and (b) Y- direction of the samples with asymmetric cross-section. .

A 3-D model of the defect structure reconstructed in the commercial software Skyscan^{TM} CT analyser was made to extract the morphometric parameters by collating the individual 2-D crossectional slices. The CT-analyser software carried out the analysis of the defects directly on a 3-D volume rendered model to determine parameters such defect volume, defect surface area and defect thickness. The result of the 3-D reconstruction of the defect structure has been shown in the figure 7. The various parameters that have been determined from the 3D reconstruction are given in table 1. From the results it can be concluded that the type of defect present near the necking region are mainly rod shaped structures of sizes that predominately lies within 2-12 μm. The overall surface to volume ratio of these structures are near to 1, which implies that they have very low sphericity. For a perfect sphere the surface to volume ratio is six. Thus it can be concluded that the void morphology present in the necked region are not like oblate spheroids but more like elongated rods. These observations of rod shaped defect structures are consistent with previous investigations on characterizing void shape developed during uni-axial deformation of steels [26, 27]. The void nucleated by cracking of carbides or by de-cohesion, initially grow predominately in the tensile direction and only at large tri-axialities does significant transverse void growth occur [26]. In the work carried out by Floreen and Hayden [26] the void size and shape (length (L) and width (W)) in annealed and aged maraging steel present as a result of uni-axial deformation were found to vary from 2-3 microns at 0.3 true strain (L/W ~ 1.5 – 2) to greater than 15 micron at 1.1 true strain (L/W ~ 3 – 4). The present investigation also shows similar rod shaped defects present in the CrMoV steel near to necking region, which were deformed upto ~0.4 true necking strain. In comparison with the earlier works [26, 27], the present investigation was able to reveal important parameters in the development of damage during ductile fracture in CrMoV steel such as size and shape range of the voids, its spatial distribution and volume fraction, which could be related to macroscopic deformation quantities such as stress and strain in the neck region. These quantities were successfully determined at lower necking strains, where the volume fraction of voids was significantly lower than 0.1% as compared with spheroidized plain carbon steels [27]. Thus the application of tomography technique using a micro-focus X-ray source has been unequivocally shown to characterize the development of damage in dense material such as structural steels as a result of uni-axial deformation and would be used in future investigations to develop functional dependence of damage parameters with respect to macroscopic stress and strain deformation environment. Further, the reasons for the small voids to anomalously increase the attenuation coefficient need to be systematically investigated.

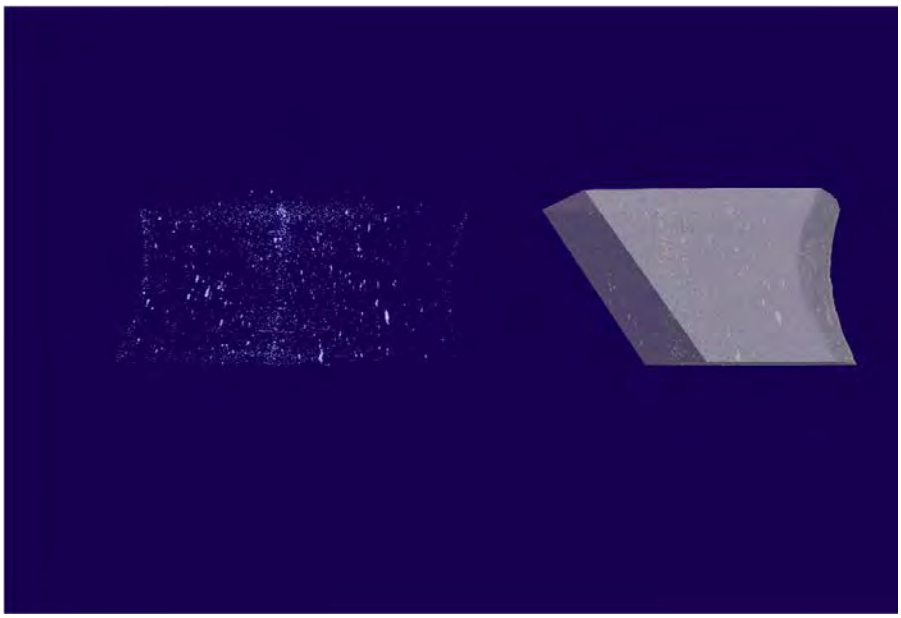

Figure 7. The spatial distribution of the defects within the volume of interest obtained from 3-D volume rendering using Skyscan™ CTAnal software.

Table 1: The defect characteristics obtained from the 3-D analysis carried out using Skyscan™ CTAn on the slice sample with rectangular cross-section.

Defect Characteristics		**Unit**	**Value**
Volume of interest (VOI)		mm^3	1.40656
Object Volume		(10^{-4}) mm^3	4.3
Object Surface		(10^{-4}) mm^2	4390.9
Surface / Volume ratio (SVR)		1/ µm	1.0311
Number of objects		nos	11261
Structure Model Index (SMI)		-	4.84[a]
Structure Thickness Distribution (Thickness Range (TR) in µm)	2 – 5	%	32
	5 – 9	%	24
	9 – 12	%	25
	12 – 16	%	14
	16 – 19	%	5
Defect Size (DS)		µm	3 – 12
Volume Fraction		%	0.03028%

a: SMI = 3 indicates that the defect are rod shaped structures.

CONCLUSION

The study shows the successful application of X-ray micro tomography using a micro-focus X-ray source to image the voids present in the necked section of a dense material such as structural steel for nuclear reactor applications. The sample shape and size seems to be an important parameter to successfully observe internal defects in steels. The integration of computed tomography to reconstruct the void structure in 3-D complements the traditional invasive methods to characterize the internal structures of materials in terms of shape, size and location distribution.

ACKNOWLEDGEMENTS

CG gratefully acknowledges Skyscan NV, Belgium for their support during the experimentation and analysis of the samples. Prof H. Toda, Dept. of Mechanical Engineering, Toyohashi University of Technology is thanked for the constant encouragements during the preparation of manuscript. Finally the Japan Society for Promotion of Science is gratefully acknowledged for financial assistance through JSPS fellowship award and grant in aid fund for scientific research (No. 22.00384).

REFERENCES

[1] Vishwanathan, R: Damage Mechanisms and Life Assessment in High Temperature Component (ASM International, Metal Park, Ohio 1989).
[2] Thomason, P. F: Ductile Fracture of Metals (Pergamon Press, Canada, 1990).
[3] Baruchel, J., Buffière, J.Y., Maire, E., Merle, P., Peix, G. "X-Ray Tomography in Material Science" HERMES Science Publications , Paris 2000.
[4] Withers, P.J., Lewandowski, J.J., "Three dimensional imaging of materials by microtomography" *Mater. Sci. Tech*. 22, 2006 pp 1009-1010.
[5] Cloetens, P., Pateyron-Salome, M., Buffière, J.Y., Peix, G.,Baruchel. J., Perin, F., Schlenker, M., "Observation of microstructure and damage in materials by phase sensitive radiography and tomography" *J. Appl. Phys*. 811997 pp 5878-5887.
[6] Hanke, R., Fuchs, T., Uhlman, N., "X-ray based method for non-destructive testing and characterization" *Nucl. Instru. Meth. Phys. Res. (A)* 591, 2008 pp 14-18.
[7] Wilkins, S.W., Gureyev, T.E., Gao, D., Pogany, A., Stevenson, A.W.,"Phase contrast imaging using polychromatic hard X-rays*" Lett. Nature* 384, 1996 pp 335-338.
[8] Wu, X., Hong, L., Amin, Y., "Phase contrast X-ray tomography: Contrast mechanism and roles of phase retrieval" *Eur. Jour. Radiol*. 68 2008 pp s8-s12.
[9] Salamon, M., Hanke, R., Krüger, P., Uhlman, N., Voland, V., "Realization of a computed tomography setup to achieve resolutions below 1 μm" *Nucl. Instru. Meth. Phys. Res. (A)* 591 2008 pp 50-53.
[10] Salamon, M., Hanke, R., Krüger, Sukowski, F., Uhlman, N., Voland, V., " Comparison of different methods for determining size of a focal spot below 1μm" *Nucl. Instru. Meth. Phys. Res. (A)* 591 2008 pp 54-58.
[11] Babout, L., " X-ray Tomographic imaging : a necessary tool for material science" *Automatyka* 10 2006 pp117-124.
[12] Babout, L., Maire, E., Buffière, J.Y., Fougeres, R., "Characterisation of X-ray computed tomography of de-cohesion, porosity growth and coalescence in model metal matrix composites" *Acta.Mater*. 49, 2001 pp 2055-2063.
[13] Buffière, J.Y., Maire, E., Cloetens, P., Leomand, G., Fougeres, R., "Characterisation of internal damage in a MMC_P using synchrotron phase contrast microtomography" *Acta. Mater*. 47 1999 pp 1613-1625.
[14] Maire, E., Gimenez, N., Moynot, V.-S., Sautereau, H., "X-ray tomography and three dimensional image analysis of epoxy glass syntactic foams" *Phil. Trans. R. Soc. A* 364 2006 pp 69-88.
[15] Savelli, S., Buffière, J.Y., Fougeres, R., "Pore characterization in a model cast aluminium alloy and its quantitative relation to fatigue studied by synchrotron X-ray microtomography" *Mat. Sci. For.* 331-337 2000 pp 197-202.
[16] Toda, H., Sinclair, I., Buffière, J.Y., Maire, E., Connolley, T., Joyce, M., Khor, K.H., Gregson, P., "Assessment of fatigue crack closure phenomenon in damage tolerant aluminium alloy by in-situ high resolution X-ray microtomography" *Philos. Mag.* 83 2003 pp 2429-2448.

[17] Buffière, J.Y., Ferrie, E., Porudon, H., Ludwig, W., "Three dimensional visualization of fatigue cracks in metals using high resolution synchrotron X-ray microtomography" *Mat. Sci. Tech*. 22 2006 pp 1019-1024.
[18] Ignatiev, K.I., Davies, G.R., Elloit, J.C., Stock, S.R., "MicroCT(microtomography) quantification of microstructure related to macroscopic behavior: Part 1 – Fatigue crack closure measured in-situ in AA2090 compact tension samples" *Mat. Sci. Tech*. 22 2006 pp 1025-1037.
[19] Breunig, T.M, Kinney, J.H., Stock, S.R., "MicroCT(microtomography) quantification of microstructure related to macroscopic behavior: Part 2 – Damage in SiC-Al monofilament composites tested in monotonic tension and fatigue" *Mat. Sci. Tech*. 22 2006 pp 1059-1067.
[20] Müller, B., Pfunder, F., Chiocca, L., Dorin Ruse, N., Beckmann, F., "Visualistion complex morphology of fatigue cracks in 3D voxel based datasets" *Mat. Sci. Tech*. 22, 2006 pp 1038-1044.
[21] Toda, H., Masuda, S., Bartes, R., Kobayashi, M., Aoyama, S., Onodera, M., Furusawa, R., Uesugi, K., Takeuchi, A., Suzuki, Y., "Statistical assessment of fatigue crack initiation from subsurface hydrogen micropores in high quality die cast aluminium", *Acta. Mater.* 59 2011 pp 4990-4998.
[22] Everett, R.K., Simmonds, K.E., Geltmacher, A.B., "Spatial distribution of voids in HY-100 steel by X-ray microtomography" *Scripta. Mater*. 44 2001 pp 165-169.
[23] Stock, S.R., "Recent advances of X-ray microtomography applied to materials" *Int. Mat. Rev*. 53 2008 pp 129-181.
[24] Toda, H., *Private Communication*.
[25] Rasband, W.S.,: ImageJ, U.S. National Institutes of Health, Bethesda Maryland, USA, http://rsb.info.nih.gov/ij/, 1997-2008.
[26] Floreen, S., Hayden, H.W., "Some observations of void growth during tensile deformation of high strength steel" *Scripta. Metall*. 4, 1970 pp 87-94.
[27] Le Roy, G., Embury, J.D., Edward, G., Ashby, M.F., "A model of ductile fracture based on nucleation and growth of voids" *Acta. Metall*. 29 1981 pp 1509-1522.